



Article

Hepatoprotective Efficacy of Cycloastragenol Alleviated the Progression of Liver Fibrosis in Carbon-Tetrachloride-Treated Mice

Theerut Luangmonkong ^{1,2} , Pittaya Puphancharoensuk ¹, Varisara Tongsongsang ¹, Peter Olinga ³
and Warisara Parichatikanond ^{1,2,*}

¹ Department of Pharmacology, Faculty of Pharmacy, Mahidol University, Bangkok 10400, Thailand

² Centre of Biopharmaceutical Science for Healthy Ageing (BSHA), Faculty of Pharmacy, Mahidol University, Bangkok 10400, Thailand

³ Department of Pharmaceutical Technology and Biopharmacy, University of Groningen, 9713 AV Groningen, The Netherlands

* Correspondence: warisara.par@mahidol.ac.th

Abstract: The continuous death of hepatocytes induced by various etiologies leads to an aberrant tissue healing process and promotes the progression of liver fibrosis and ultimately chronic liver diseases. To date, effective treatments to delay this harmful process remain an unmet clinical need. Cycloastragenol is an active phytochemical substance isolated from *Astragalus membranaceus*, a plant used in traditional Chinese medicine to protect the liver. Therefore, our study aimed to elucidate the efficacy of cycloastragenol on carbon-tetrachloride (CCl₄)-induced liver fibrosis in mice. We found that cycloastragenol at 200 mg/kg dosage exhibited anti-fibrotic efficacy as demonstrated by a decrease in collagen deposition, downregulation of mRNA expression of collagen type 1, and a reduction in the content of total collagens. In addition, cycloastragenol further augmented the levels of anti-fibrotic matrix metalloproteinases (Mmps), that is, Mmp8, proMmp9, and Mmp12, which play a pivotal role in fibrosis resolution. According to histological analysis and serum markers of hepatotoxicity, cycloastragenol protected the livers from damage and mitigated the increment of serum alanine aminotransferase and bilirubin implicating hepatoprotective efficacy against CCl₄. Moreover, cycloastragenol upregulated the mRNA expression of interleukin 6, a pleiotropic cytokine plays a vital role in the promotion of hepatocyte regeneration. In conclusion, cycloastragenol alleviated the progression of liver fibrosis in CCl₄-treated mice and its anti-fibrotic efficacy was mainly due to the hepatoprotective efficacy.

Keywords: cycloastragenol; CCl₄; liver fibrosis; hepatoprotection; fibrosis resolution



Citation: Luangmonkong, T.; Puphancharoensuk, P.; Tongsongsang, V.; Olinga, P.; Parichatikanond, W. Hepatoprotective Efficacy of Cycloastragenol Alleviated the Progression of Liver Fibrosis in Carbon-Tetrachloride-Treated Mice. *Biomedicines* **2023**, *11*, 231. <https://doi.org/10.3390/biomedicines11010231>

Academic Editor: Jun Lu

Received: 23 December 2022

Revised: 12 January 2023

Accepted: 13 January 2023

Published: 16 January 2023



Copyright: © 2023 by the authors. Licensee MDPI, Basel, Switzerland. This article is an open access article distributed under the terms and conditions of the Creative Commons Attribution (CC BY) license (<https://creativecommons.org/licenses/by/4.0/>).

1. Introduction

Repeated hepatic cell deaths resulting from chronic inflammation and oxidative stress lead to an aberrant tissue healing process which could promote liver fibrosis and ultimately chronic liver diseases. Persistent liver injury can be induced by various etiologies such as viruses [1], alcohol [2], drugs [3], cholestasis [4], and steatosis [5]. Following the necrosis and apoptosis of hepatocytes, these harmful contributors commence a series of events including the activation of quiescent hepatic stellate cells (HSCs) into fibrogenic myofibroblasts which induce excessive extracellular matrix (ECM) accumulation, especially fibrillar collagen type 1 [6,7]. In fact, ECM can be properly degraded leading to fibrosis resolution by enzyme matrix metalloproteinases (Mmps); however, an imbalance between the process of deposition and degradation may alter the composition of ECM proteins which eventually lead to scar formation and dysfunction of the affected liver tissue [8]. Besides necrosis and apoptosis, chronic inflammation and oxidative stress may trigger compensatory proliferation of mature hepatocytes and telomere shortening. As a result, hepatocytes are senescent, and liver regeneration is defective [9]. In the pathogenesis of liver fibrosis, these processes are regulated by several profibrogenic cytokines; however,

the transforming growth factor-beta 1 (TGF- β 1) signaling plays a pivotal role since it is responsible for the activation of myofibroblasts and the regulation of ECM homeostasis [10].

Cycloastragenol is an active phytochemical substance in *Astragalus membranaceus* (Fisch.) Bunge, huang qi, a plant used in traditional Chinese medicine to improve immune functions and protect the liver [11]. Several attractive pharmacological properties of cycloastragenol which might contribute to the beneficial effects on the liver including hepatoprotective efficacy, antioxidative and anti-inflammatory properties, and telomerase activation to elongate telomere, have been demonstrated [11]. Recently, a previous study in rats revealed that astragaloside, which is the parent compound of cycloastragenol prior to the hydrolysis process, could prevent bile duct ligation-induced liver fibrosis via the modulation of notch signaling [12]. In addition, a similar study in rats demonstrated that a combination of total astragalus saponins and glycyrrhizic acid alleviated both bile duct ligation and dimethylnitrosamine-induced liver fibrosis via the modulation of TGF- β 1 pathways [13]. Nevertheless, the potency of cycloastragenol which is believed to be the biological active component of astragaloside on the amelioration of liver fibrosis induced by hepatotoxins are currently unknown. Therefore, our study aimed to elucidate the efficacy of cycloastragenol on carbon-tetrachloride (CCl₄)-induced liver fibrosis in mice. Beyond anti-fibrotic potency, the effects of cycloastragenol on hepatoprotection, inflammation, oxidative stress, telomere length, and TGF- β 1-related signaling were elucidated to explore the associated mechanism of action.

2. Materials and Methods

2.1. Animals

Male ICR outbred mice at 6 weeks old were purchased from the National Laboratory Animal Center, Nakhon Pathom, Thailand. The mice were housed in a temperature and humidity-controlled room with a 12 h light/dark cycle. The standard rodent diet and filtered water were supplied ad libitum. The study commenced after an acclimatization period of the mice in the housing room for at least 7 days. This study, which complied with the ARRIVE (Animal Research: Reporting of In Vivo Experiments) guidelines [14], was approved by the Animal Ethical Committee of the Faculty of Pharmacy, Mahidol University (PYR002/2021 and PYR008/2022).

2.2. Experimental Protocol

The mice were randomly divided into 4 groups (n = 10 per group, 40 mice in total): (1) normal, (2) control, (3) cycloastragenol 50 mg/kg, and (4) cycloastragenol 200 mg/kg. To induce liver fibrosis, mice in groups 2–4 were administered CCl₄ (Shanghai Seasonsgreen Chemical, Shanghai, China) by intraperitoneal injection twice a week for a consecutive 8 weeks. The amount of CCl₄ was gradually escalated from 0.03 mL/kg, 0.075 mL/kg, and 0.1 mL/kg in the 1st, 2nd, and 3rd weeks, respectively. During the 4th to 8th weeks, CCl₄ was administered at 0.12 mL/kg. Prior to the administration, CCl₄ was diluted in olive oil to inject with an equivalent volume according to the individual body weight of each mouse. Starting from the 5th week until the 8th week, cycloastragenol (King-tiger Pharm-Chem, Chendu, China), prepared by dispersing in 0.5% sodium carboxymethylcellulose, was given to the mice in groups 3 and 4 by oral gavage once a day for 5 days per week. The mice in group 2 were administered olive oil and 0.5% sodium carboxymethylcellulose in an equivalent amount was administered to groups 3 and 4. At 72 h after receiving the last dosage of CCl₄, the mice were anesthetized using carbon dioxide before terminal cardiac puncture for blood collection until complete euthanization. Before the isolation, the livers were thoroughly perfused using 0.9% sodium chloride solution via the portal vein until there was no residual blood. The isolated liver was separated into several pieces for fixing in 10% neutral-buffered formalin and snap-freezing in liquid nitrogen for further assays.

2.3. Histological Evaluations

The median lobes of livers, preliminarily fixed in 10% neutral-buffered formalin for at least 48 h, were processed in a series of ethanol and xylene and embedded in paraffin. The 4 μ m liver sections were stained with picro-sirius red to determine collagen fiber deposition [15]. In addition, another section of the same piece of livers was stained with hematoxylin/eosin for routine histopathological examination to evaluate the histological damage score, assessed from the degree of hepatocyte degenerations, necrobiotic changes, and infiltrated lymphocytes by a described method [16]. The sections were examined using an electric light microscope (Olympus IX-81, Tokyo, Japan). To analyze microscopical pictures, 5 random non-overlapping frames per liver were selected for the analysis using ImageJ (National Institutes of Health, Bethesda, MD, USA).

2.4. Serum Biomarker Measurements

The clotted blood was centrifuged at $10,000\times g$ for 10 min to collect serum. The levels of liver-related injury markers, that is, alanine aminotransferase, aspartate aminotransferase, alkaline phosphatase, total and direct bilirubin, total protein, and albumin, were immediately quantified using an automated serum biochemical analyzer (Olympus AU400 Chemistry Analyzer, Tokyo, Japan) with the supplied diagnosis reagent kits.

2.5. Hepatic Hydroxyproline Assay

To quantify total hepatic collagens, a colorimetric assay to detect hydroxyproline, which is a unique modified-amino acid that is mostly found in collagens, was performed by a minor modification of the described procedure [17]. In brief, an exact weight of the snap-frozen liver (approximately 100 mg) taken from 2 different lobes was homogenized in 6 N hydrochloric acid and hydrolyzed at 95 °C for 16 h. The hydrolyzed samples were centrifuged and the supernatants were mixed with chloramine-T solution in citrate-acetate buffer pH 6.0 and isopropanol before being incubated in Ehrlich's reagent (*p*-dimethylamino-benzaldehyde, perchloric acid, and isopropanol) at 60 °C for 1 h. The colorimetric product of the reaction was measured with a Synergy HT spectrophotometer (Agilent, Santa Clara, CA, USA) at 550 nm. The content of hydroxyproline in each sample was reported as μ g hydroxyproline per 100 mg of liver or per the whole liver.

2.6. Total RNA and Genomic DNA Isolation

Total RNA and genomic DNA were isolated from a piece of snap-frozen livers (approximately 30 mg) acquired from the same lobe using the AllPrep DNA/RNA/Protein MiniKit (Qiagen, Venlo, The Netherlands). The quantification and qualification of RNA and DNA were measured using a Nanodrop One spectrophotometer (Thermo Fisher Scientific, Waltham, MA, USA). The isolated total RNA was consequently reverse-transcribed prior to a quantitative real-time polymerase chain reaction (PCR) and an RNA profiler for the evaluation of gene expression. The isolated genomic DNA was used to quantify the telomere length.

2.7. Evaluation of Gene Expression

Reverse transcription was performed using an RT² First Strand Kit (Qiagen). In brief, the isolated RNA was initially incubated with a genomic DNA-eliminating buffer at 42 °C for 5 min. The DNA-eliminated RNA was reverse-transcribed at 42 °C for 15 min before stopping the reaction at 95 °C for 5 min.

Gene expression was determined using specific primers (Table 1) and a Brilliant III Ultra-Fast SYBR Green QRT-PCR Master Mix (Agilent) on a CFX96 Real-Time PCR Detection System (Biorad, Irvine, CA, USA) with a cycle at 50 °C for 10 min and at 95 °C for 3 min followed by 40 cycles of 95 °C for 15 s and 60 °C for 30 s. Expression levels were corrected using glyceraldehyde-3-phosphate dehydrogenase (GAPDH) as a reference gene (dCt) and compared with the control group (ddCt). The results are displayed as a fold induction ($2^{-\text{ddCt}}$).

Table 1. Primer sequences used for quantitative real-time PCR.

Genes	Forward Primers (5'–3')	Reverse Primers (5'–3')
<i>Bad</i>	CTCCGAAGGATGAGCGATGAG	CTCCGAAGGATGAGCGATGAG
<i>Cat</i>	GGAGGCGGGAACCCAATAG	GGAGGCGGGAACCCAATAG
<i>Col1a1</i>	TGACTGGAAGAGCGGAGAGT	ATCCATCGGTCATGCTCTCT
<i>Gapdh</i>	ACAGTCCATGCCATCACTGC	GATCCACGACGGACACATTG
<i>Gpx1</i>	CCACCGTGTATGCCTTCTCC	AGAGAGACGCGACATTCTCAAT
<i>Gsr</i>	CACGGCTATGCAACATTCGC	GTGTGGAGCGGTAAACTTTTTT
<i>Igf</i>	TCGTGGGATGGGTGCTTT	TGAAGACAGTAGGGAAGAGACAAG
<i>Il6</i>	TCCATCCAGTTGCCTTCT	TAAGCCTCCGACTTGTGAA
<i>Nqo1</i>	AGGATGGGAGGTACTCGAATC	TGCTAGAGATGACTCGGAAGG
<i>Nrf2</i>	CTGAACTCCTGGACGGGACTA	CGGTGGGTCTCCGTAATGG
<i>Ppara</i>	CACCTTGCTCACTACTGTCCTT	GATGCTGGTATCGGCTCAA
<i>Pparγ</i>	GGTGCTCCAGAAGATGACAGA	TCAGCGGTGGGACTTTT
<i>Sod1</i>	AACCAGTTGTGTTGTCAGGAC	CCACCATGTTTCTTAGAGTGAGG
<i>Sod2</i>	TGGACAAACCTGAGCCCTAAG	CCCAAAGTCACGCTTGATAGC
<i>Tgf-β1</i>	GGTTCATGTCATGGATGGTGC	TGACGTCCTGAGTTGTACGG

RT² Profiler™ PCR Array Mouse Fibrosis (Qiagen, GeneGlobe ID: PAMM-120Z) with preloaded primers in 100-well strips were used to elucidate 84 genes related to fibrosis. cDNA was mixed with a 2X RT² SYBR Green ROX FAST Mastermix (Qiagen). Thermal cycling and fluorescence detection were performed on a Rotor-Gene Q (Qiagen) with a cycle of 95 °C for 10 min followed by 40 cycles of 95 °C for 15 s and 60 °C for 30 s. Expression levels were corrected using GAPDH as a reference gene. The results are displayed as the magnitude of gene expression when compared with normal using the company's program for generating a heat-map clustrogram.

2.8. Quantification of Telomere Length

Telomere length was measured using a Relative Mouse Telomere Length Quantification qPCR Assay Kit (Sciencell Research Laboratory, Carlsbad, CA, USA). In brief, the genomic DNA was mixed with a 2X GoldNStart TaqGreen qPCR master mix containing a primer set designed to recognize and amplify a specific part of telomere sequences. The single copy reference, designed to recognize and amplify a region on chromosome 10, was used for data normalization. The data are shown as relative telomere length when compared with the normal length using $2^{-\text{ddCt}}$ method.

2.9. Evaluation of Protein Expression

The expression of multiple Mmps and proteins associated with TGF- β 1-related signaling was quantified using Milliplex immunoassay (Merck, Rahway, NJ, USA), a bead-based multiplex enzyme-linked immunosorbent assay (ELISA) which could analyze multiple target proteins simultaneously. In brief, a piece of snap-frozen livers (approximately 30 mg) acquired from the same lobe was homogenized in kit-supplied lysis buffer containing a phosphatase inhibitor with supplement of Protease Inhibitor Cocktail Set III (Calbiochem, San Diego, CA, USA). After the centrifugation of liver homogenate, the amount of target proteins in the supernatant was quantified using a specific conjugated antibody with a designed magnetic bead technology. The value of proteins was normalized using total protein content measured by a Pierce™ BCA Protein Assay Kit (Thermo Fisher Scientific).

2.10. Statistic

Data are expressed as means + standard error of the mean (SEM) of numerical results among the same treatment. The statistical tests on the means of different groups were performed using one-way analysis of variance (ANOVA) followed by Tukey's multiple comparisons. Prism 6.01 (GraphPad Software, San Diego, CA, USA) was the software used for the statistical calculation. A *p*-value less than 0.05 was considered significant. For gene expression and relative telomere length, the statistical differences were determined on ddCt.

Since some mice died during the induction of fibrosis, the number of animals per group at the end of experiment was 8–10.

3. Results

3.1. Anti-Fibrotic Efficacy

To evaluate the anti-fibrotic potency of cycloastragenol, fibrillar collagens by picrosirius red staining, expression of collagen type 1 mRNA (*Col1a1*) by quantitative real-time PCR, and content of total collagens by hydroxyproline assay were performed (Figure 1). We found that fibrillar collagens were increasingly deposited in the livers of mice treated with CCl₄. Similarly, at the gene level and the total content of collagens in the livers, CCl₄ upregulated the expression of *Col1a1* and increased the hydroxyproline content, respectively. Based on all collagen-associated analyses, cycloastragenol at 200 mg/kg dosage exhibited anti-fibrotic efficacy in the liver of CCl₄-treated mice as demonstrated by a decrease in collagen deposition, downregulation of *Col1a1* expression, and a reduction in the content of total collagens. In contrast, the anti-fibrotic efficacy of cycloastragenol at 50 mg/kg was not apparently observed, especially on the picro-sirius red staining and *Col1a1* expression. Therefore, the 200 mg/kg of cycloastragenol appeared to be the effective dosage, and the efficacy of this dosage was shown in the other analyses of our study.

Next, we screened the effects of cycloastragenol against CCl₄ on the expression of 84 genes associated with fibrosis by using the PCR array and found that cycloastragenol may probably affect various pathways in the alleviation of liver fibrogenesis (Figure 2). Highlighted examples were the decreased expressions of collagen type 1-alfa 2 chain (*Col1a2*), collagen type 3 (*Col3a1*), and collagen maturation enzyme lysyl oxidase (*Lox*). Multiple subtypes of integrins (*Itga3*, *Itgb5*, *Itga1*, *Itgav*, *Itgb6*, *Itgb8*, and *Itgb1*) and integrin-linked kinase (*Ilk*) which are responsible for cell–cell and cell–ECM interactions were downregulated. In addition, cycloastragenol reduced the expression of the gene-encoding tissue inhibitor of metalloproteinases (*Timp1*, *Timp2*, and *Timp4*) while it increased the expression of Mmps (*Mmp3* and *Mmp9*). Beyond ECM-related genes, cycloastragenol also downregulated the expression of pro-inflammatory markers, such as chemokine ligands (*Ccl3*, *Ccl12*, and *Ccl11*), chemokine receptor 2 (*Ccr2*), interleukins (*Il1a* and *Il1b*), and signaling proteins (*Stat1* and *Nfkb1*). Vice versa, anti-inflammatory cytokines (*Il4*, *Il10*, and *Il13*) were upregulated. Furthermore, the expressions of markers related with TGF-β1 signaling-related markers (*Tgfbr2*, *Smad2*, *Tgfb1*, *Tgfb2*, *Ltbp1*, and *Tgif1*) and cell death (*Bcl2*, *Myc*, *Jun*, and *Akt1*) were decreased. Nonetheless, some markers (such as *Tnf*, *Il5*, *Pdgfa*, *Pdgfb*, and *Smad4*) were unexpectedly increased. Thus, other techniques were subsequently performed to elucidate the associated mechanism of cycloastragenol on fibrogenesis.

Since the screening of genes relating to ECM remodeling was affected by cycloastragenol, the multiplex ELISA was used to assess the level of Mmps in the liver (Figure 3). We found that CCl₄ obviously increased the expression of *Mmp2*, *Mmp8*, pro*Mmp9*, and *Mmp12*. Superior to the levels in the control group, cycloastragenol further augmented the levels of *Mmp8*, pro*Mmp9*, and *Mmp12*, indicating the elevation of fibrosis resolution.

3.2. Hepatoprotective Efficacy

The hepatocyte degenerations, necrobiotic changes, and infiltrated lymphocytes of the livers were assessed using hematoxylin/eosin staining (Figure 4). The histological analysis revealed that CCl₄ induced a high degree of liver damage as seen by the spread of ballooning hepatocytes with condensed chromatin in the enlarged nucleus and infiltrated lymphocytes in the central area of the hepatic lobules. Significantly, cycloastragenol alleviated the harmful effects of CCl₄; however, liver damage remained visible at a lower degree when compared with the control.

In line with the histological analysis, CCl₄ evidently induced liver damages resulting in an increment in liver enzymes, especially alanine aminotransferase, in the serum. Moreover, the mice treated with CCl₄ appeared to incite an impairment of liver function as seen by the increment of bilirubin, a waste biological product to be excreted by the

liver (Figure 5). Cycloastragenol tended to mitigate the increment of serum liver enzymes, alanine aminotransferase, aspartate aminotransferase, alkaline phosphatase, and bilirubin, both measured as total (conjugated and unconjugated) and direct (conjugated). Thus, cycloastragenol elicited hepatoprotective efficacy and preserved liver function against CCl_4 .

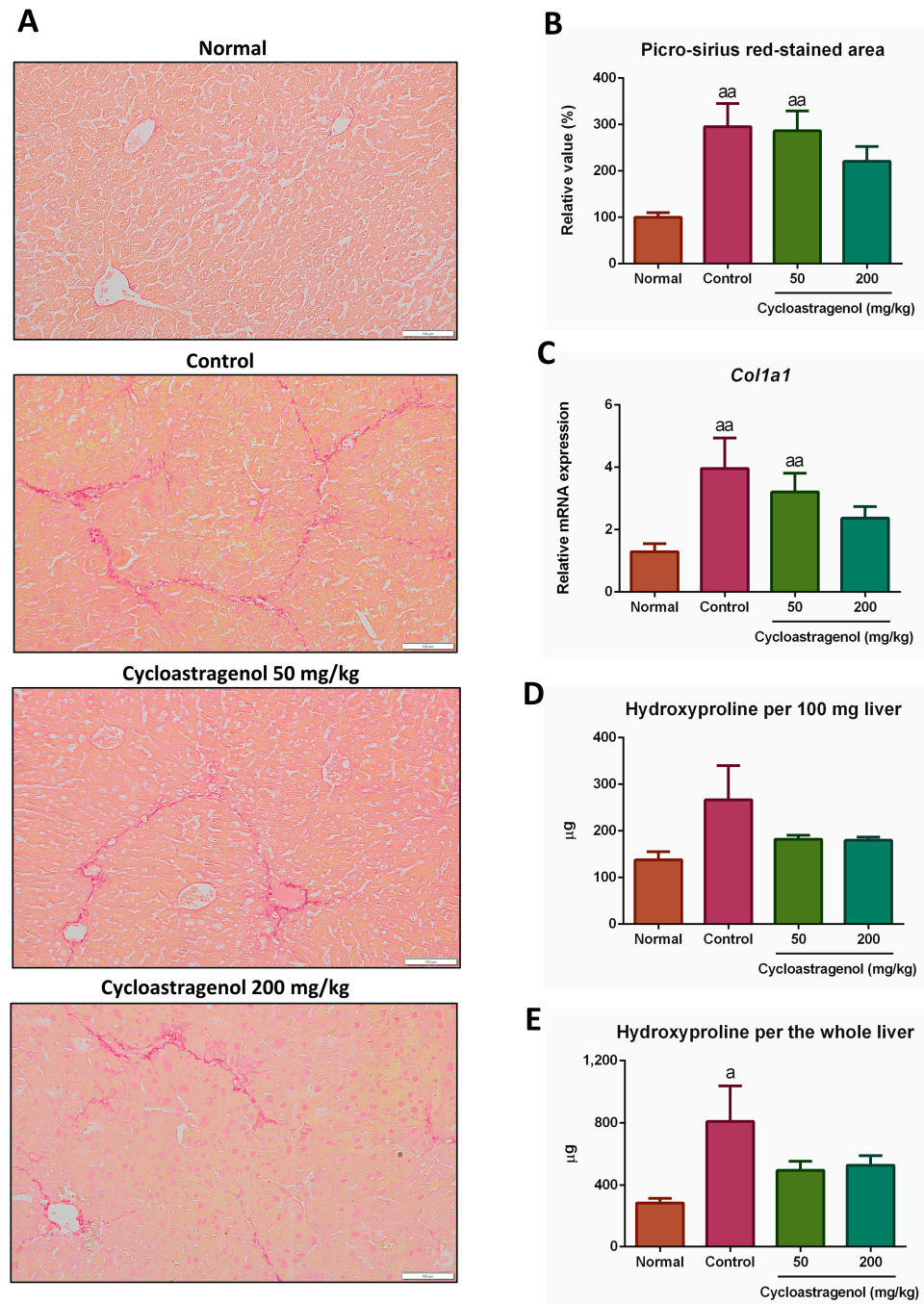


Figure 1. Anti-fibrotic efficacy of cycloastragenol (50 mg/kg and 200 mg/kg) in the liver of mice treated with carbon-tetrachloride. Representative picro-sirius red-stained pictures of the liver among each group (A) are shown. The stained areas of picro-sirius red (B) and relative mRNA expression of collagen type 1 (*Col1a1*, (C)) when compared with the normal are shown. Hydroxyproline contents of the liver when calculated per 100 mg liver tissue (D) and per the whole liver (E) are shown. Scaled bar = 100 µm. Bar graphs and corresponding error bars indicate means and SEM among the same treatment, respectively ($n = 8-10$). ^a and ^{aa} indicate $p < 0.05$ and 0.01 when compared with the normal, respectively.

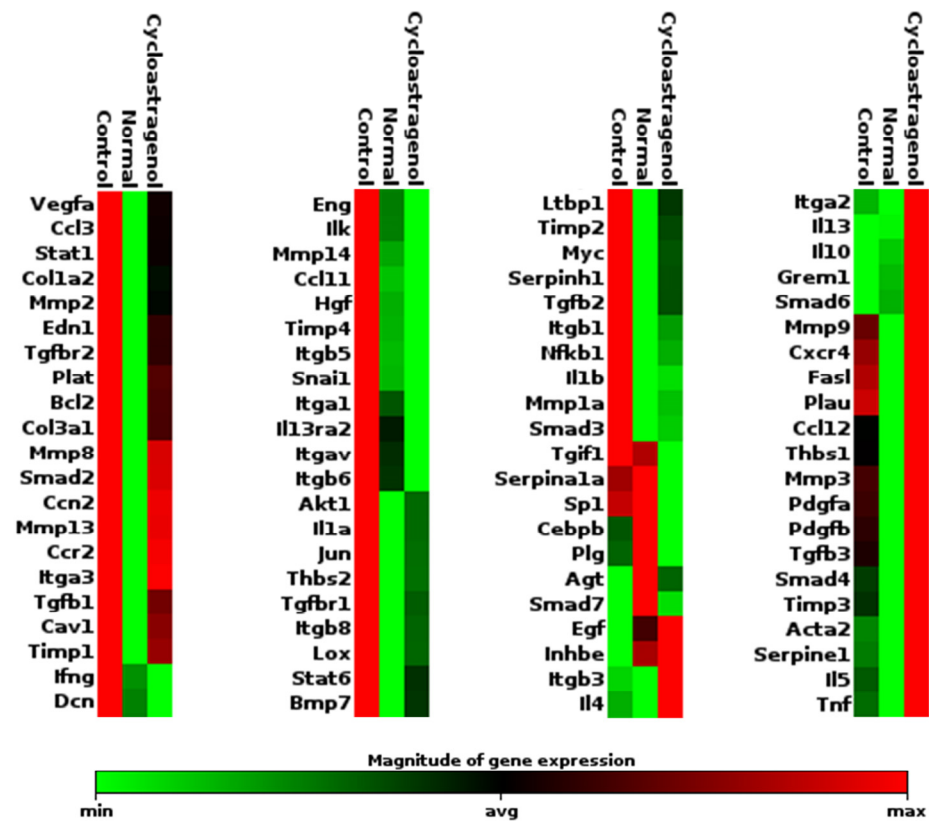


Figure 2. Effects of cycloastragenol (200 mg/kg) on the expression 84 fibrosis-related genes in the liver of mice treated with carbon-tetrachloride. Relative mRNA expression of each gene when compared with the normal are indicated using arrays of colors in a heat-map clustogram, representing a sample among each group, is shown.

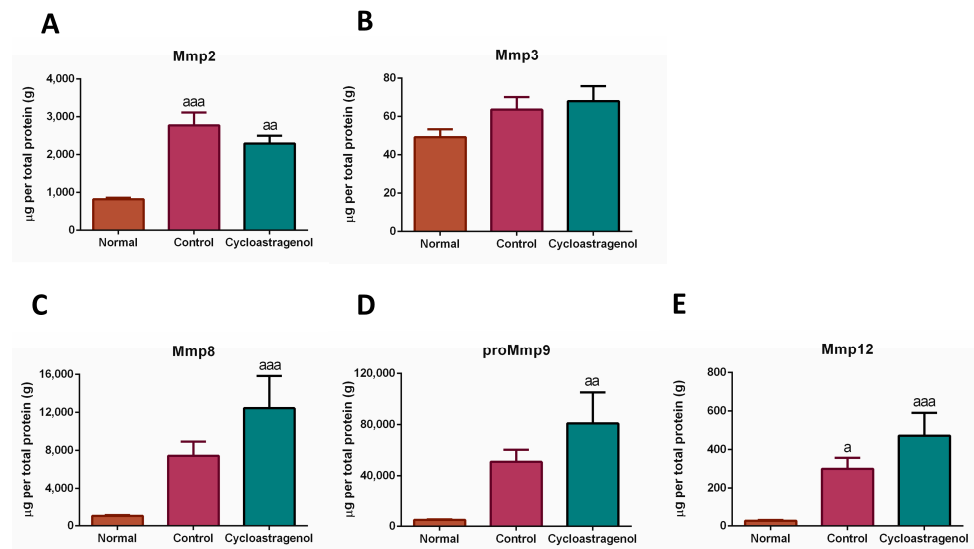


Figure 3. Effects of cycloastragenol (200 mg/kg) on the level of matrix-metalloproteinases (Mmps) in the liver of mice treated with carbon-tetrachloride. Data are expressed as the levels of Mmp2 (A), Mmp3 (B), Mmp8 (C), proMmp9 (D), and Mmp12 (E), per total protein content of the liver (g). Bar graphs and corresponding error bars indicate means and SEM among the same treatment, respectively ($n = 8-10$). ^a, ^{aa}, and ^{aaa} indicate $p < 0.05$, 0.01 , and 0.001 when compared with the normal, respectively.

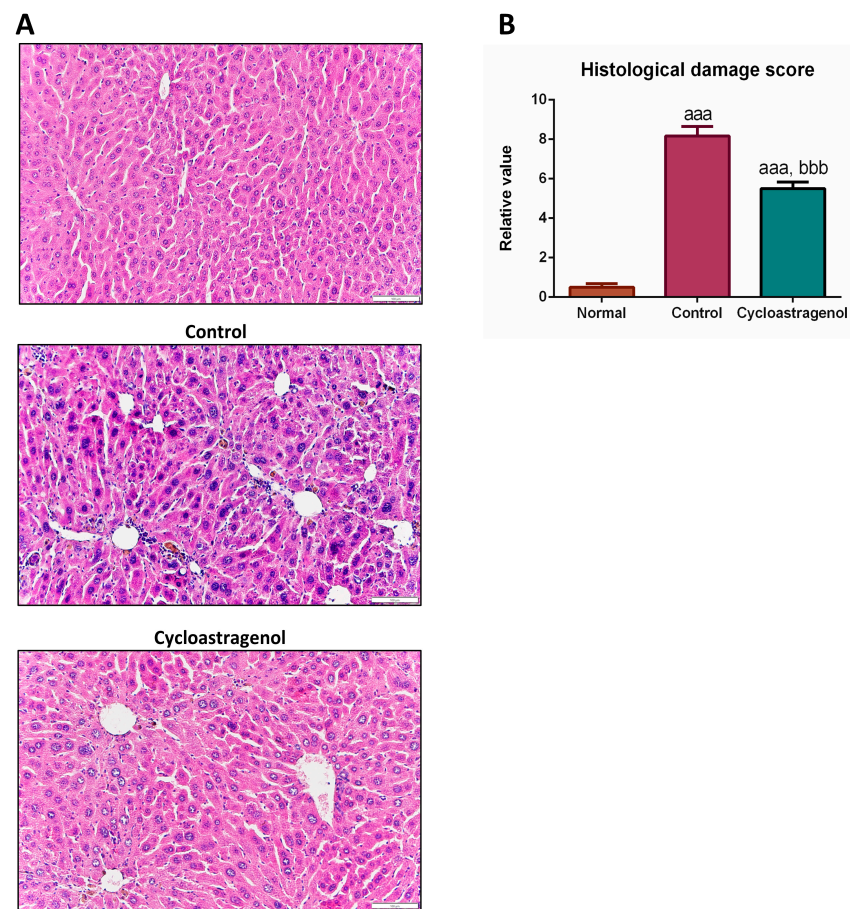


Figure 4. Hepatoprotective efficacy of cycloastragenol on histological damages in the liver of mice treated with carbon-tetrachloride. Representative hematoxylin/eosin-stained pictures of the liver among each group (A). The degree of hepatocyte degenerations, necrobiotic changes, and infiltrated lymphocytes were semi-quantified as histological damage scores. Data are shown when compared with the normal (B). Scaled bar = 100 μ m. Bar graphs and corresponding error bars indicate means and SEM among the same treatment, respectively ($n = 8-10$). ^{aaa} and ^{bbb} indicate $p < 0.001$ when compared with the normal and control, respectively.

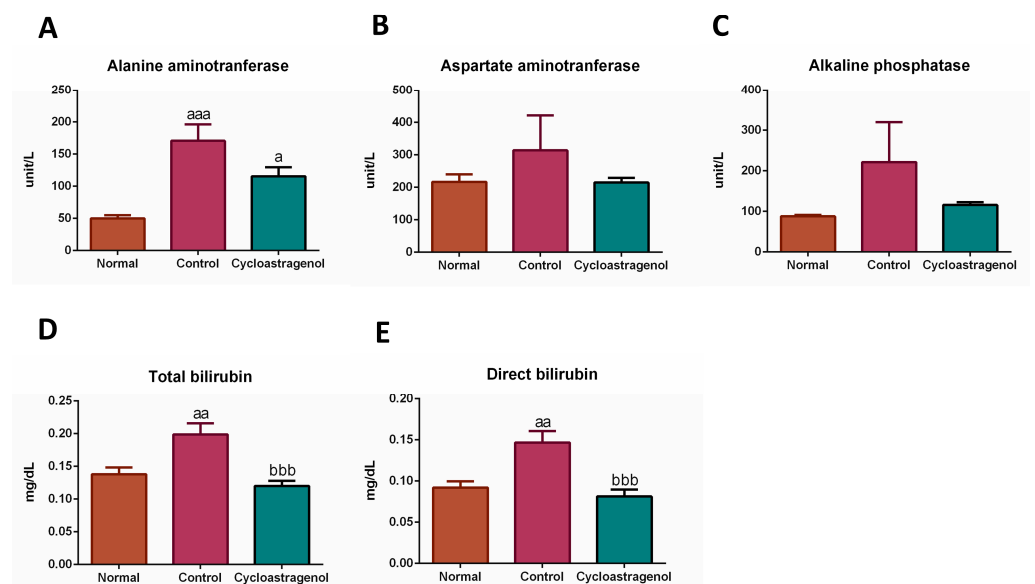


Figure 5. Cont.

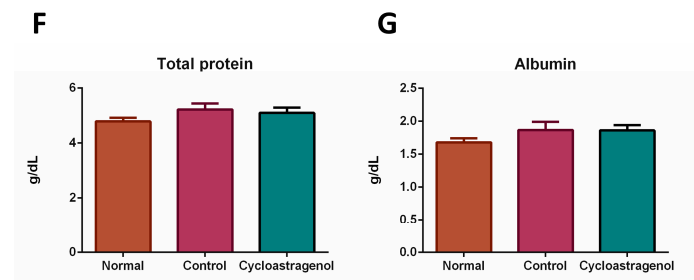


Figure 5. Hepatoprotective efficacy of cycloastragenol (200 mg/kg) on the levels of markers associated with liver toxicity in the serum of mice treated with carbon-tetrachloride. Levels of alanine aminotransferase (A), aspartate aminotransferase (B), alkaline phosphatase (C), total bilirubin (D), direct bilirubin (E), total protein (F), and albumin (G) are shown. Bar graphs and corresponding error bars indicate means and SEM among the same treatment, respectively ($n = 8-10$). ^a, ^{aa}, and ^{aaa} indicate $p < 0.05$, 0.01 , and 0.001 when compared with the normal, respectively. ^{bbb} indicates $p < 0.001$ when compared with the control.

3.3. Anti-Inflammatory, Antioxidative, and Anti-Senescent Efficacy

To investigate the mechanisms underlying hepatoprotective efficacy of cycloastragenol, several markers associated with inflammation, oxidative stress, and senescence were quantified. Among inflammatory-related markers, the mRNA expression of anti-inflammatory cytokine interleukin 6 (*Il6*) in the liver of mice who received CCl_4 alone was significantly downregulated (Figure 6). In the mice who received cycloastragenol, the expression of *Il6* was recovered to be at the same level as expressed in normal mice. We could not detect an obvious alteration on other inflammatory-related markers, that is, insulin-like growth factor (*Igf*), peroxisome proliferator-activated receptor alpha (*Ppara*), and peroxisome proliferator-activated receptor gamma (*Ppar* γ).

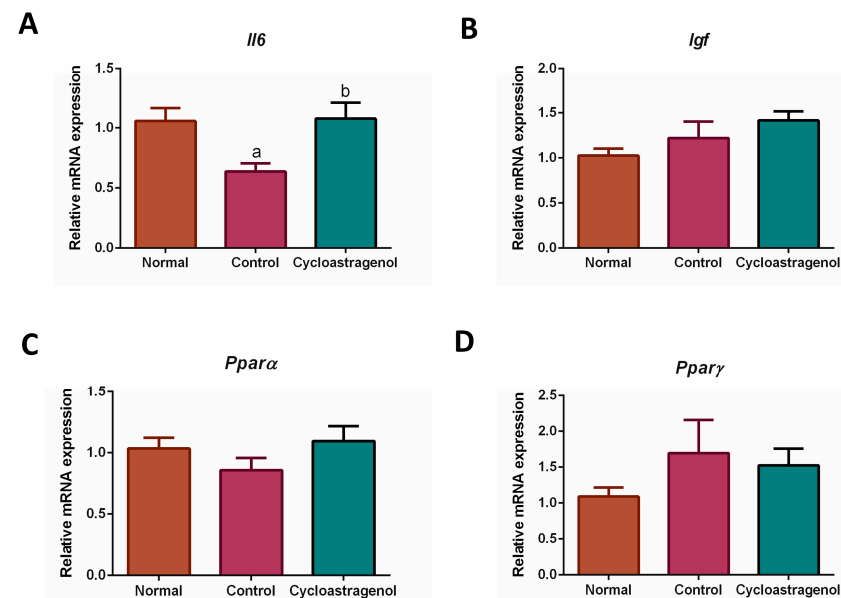


Figure 6. Effects of cycloastragenol (200 mg/kg) on the expression of gene-encoding markers associated with inflammation in the liver of mice treated with carbon-tetrachloride. Relative mRNA expression of interleukin 6 (*Il6*, (A)), insulin-like growth factor (*Igf*, (B)), peroxisome proliferator-activated receptor alpha (*Ppara*, (C)), and peroxisome proliferator-activated receptor gamma (*Ppar* γ , (D)) when compared with the normal is shown. Bar graphs and corresponding error bars indicate means and SEM among the same treatment, respectively ($n = 8-10$). ^a and ^b indicate $p < 0.05$ when compared with the normal and control, respectively.

Focusing on antioxidative efficacy, we found that the gene expression of NAD(P)H quinone dehydrogenase 1 (*Nqo1*) was the most apparently upregulated in response to CCl_4 (Figure 7). However, this cytoprotective enzyme was not remarkably affected by cycloastragenol. Besides the statistically insignificant alteration of the mRNA expression of nuclear factor erythroid 2-related factor 2 (*Nrf2*), the expression of genes encoding other enzymes responsible for scavenging reactive species was not significantly regulated by either CCl_4 or cycloastragenol.

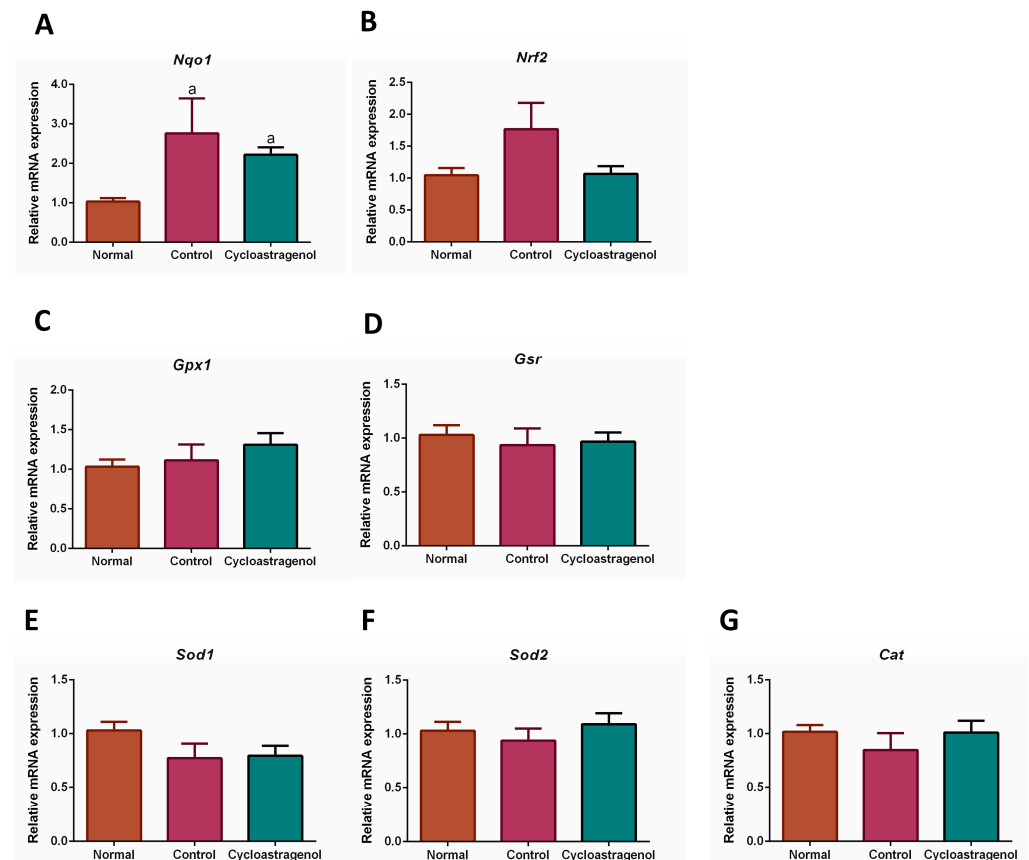


Figure 7. Effects of cycloastragenol (200 mg/kg) on the expression of gene-encoding markers associated with oxidative stress in the liver of mice treated with carbon-tetrachloride. Relative mRNA expression of NAD(P)H quinone dehydrogenase 1 (*Nqo1*, (A)), nuclear factor erythroid 2-related factor 2 (*Nrf2*, (B)), glutathione peroxidase 1 (*Gpx1*, (C)), glutathione-disulfide reductase (*Gsr*, (D)), superoxide dismutase 1 (*Sod1*, (E)), superoxide dismutase 2 (*Sod2*, (F)), and catalase (*Cat*, (G)) when compared with the normal is shown. Bar graphs and corresponding error bars indicate means and SEM among the same treatment, respectively ($n = 8-10$). ^a indicates $p < 0.05$ when compared with the normal.

The gene expression of a senescent marker Bcl2-associated agonist of cell death (*Bad*) was not obviously increased in response to CCl_4 (Figure 8). Thus, although the level was comparable to the normal, we could not conclude that cycloastragenol exhibited anti-senescent efficacy. This finding was in line with the length of telomere in the genomic DNA of mice treated with CCl_4 and cycloastragenol.

3.4. Effects on TGF- β 1 Signaling Pathway

Since the screening of gene expression revealed that several TGF- β 1 signaling-related markers were affected by cycloastragenol, quantitative real-time PCR of TGF- β 1 ligand (*Tgf- β 1*) was conducted and the multiplex ELISA was used to assess the level of TGF- β 1 signaling-related proteins in the liver (Figure 9). We found that CCl_4 tended to increase the expression of *Tgf- β 1* and phosphorylated protein kinase B (pAkt); however, the increments were not significantly higher than the normal or mice who received cycloastragenol. The

expression of other TGF- β 1 signaling-related markers was not remarkably changed by either CCl₄ or cycloastragenol.

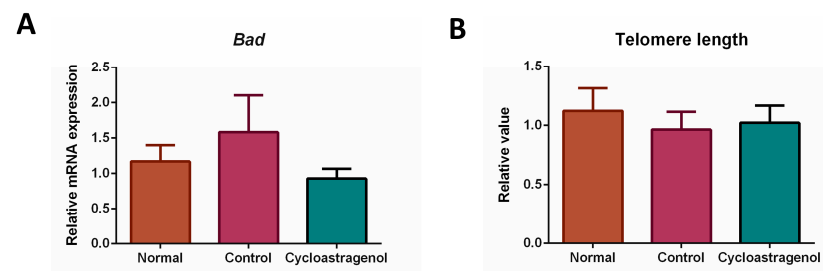


Figure 8. Effects of cycloastragenol (200 mg/kg) on the markers of senescence in the liver of mice treated with carbon-tetrachloride. Relative Bcl2-associated agonist of cell death (*Bad*) mRNA expression (A) and telomere length of genomic DNA (B) when compared with the normal are shown. Bar graphs and corresponding error bars indicate means and SEM among the same treatment, respectively ($n = 8–10$).

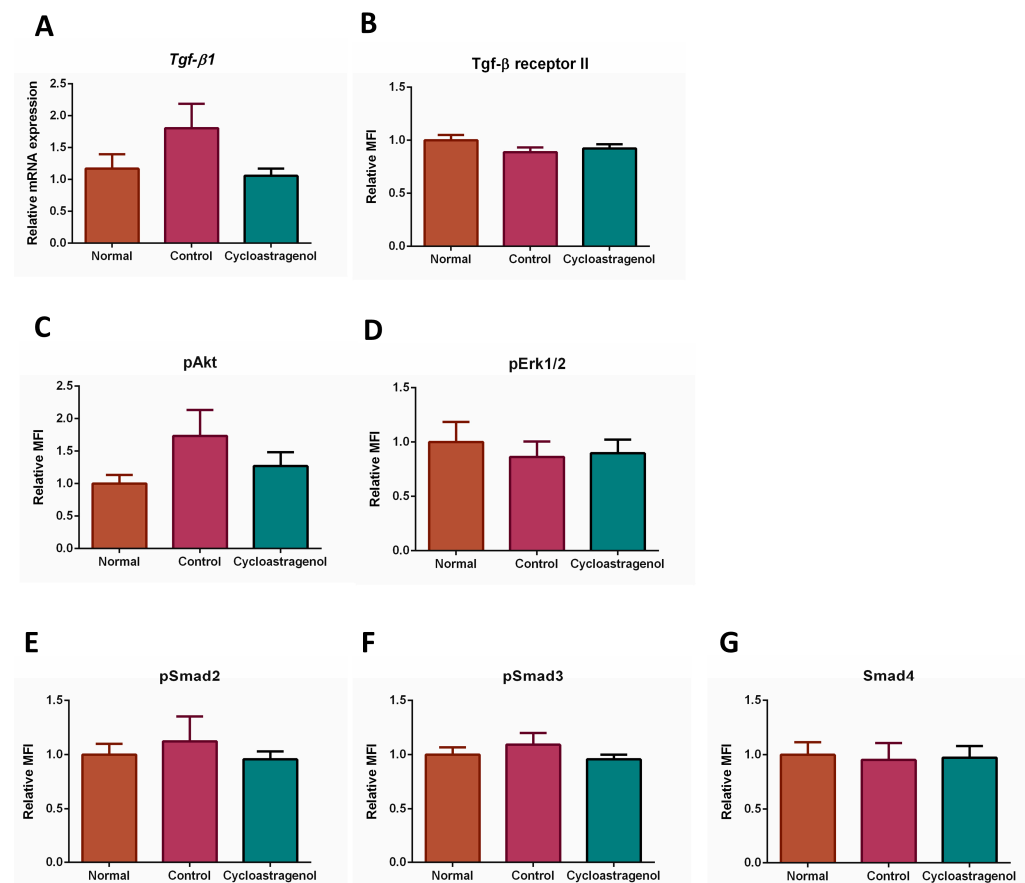


Figure 9. Effects of cycloastragenol (200 mg/kg) on the expression of markers associated with transforming growth factor-beta 1 (TGF- β 1) signaling in the liver of mice treated with carbon-tetrachloride. Relative mRNA expression of TGF- β 1 (*Tgf- β 1*, (A)) and relative median fluorescence intensity (MFI) of transforming growth factor-beta receptor II (Tgf- β receptor II, (B)), phosphorylated protein kinase B (pAkt, (C)), phosphorylated extracellular signal-regulated kinase 1/2 (Erk1/2, (D)), phosphorylated-Smad2 (pSmad2, (E)), phosphorylated-Smad3 (pSmad3, (F)), and Smad4 (G) when compared with the normal are shown. Bar graphs and corresponding error bars indicate means and SEM among the same treatment, respectively ($n = 8–10$).

4. Discussion

To date, the sole therapeutic option for patients with advanced chronic liver diseases is liver transplantation. Nonetheless, this invasive and high-risk surgical procedure is sufficient for a limited number of patients [18]. Therefore, effective treatments remain an unmet clinical need. Among available options, the eradication of underlying causes which prevail the death of hepatocytes by using antiviral therapy for chronic hepatitis B and C infection could be considered the most effective treatment because the drugs can prevent or even reverse the progression of disease [19]. In traditional Chinese medicine, *Astragalus membranaceus* (Fisch.) Bunge has been used in various preparations to protect the liver from harmful causes for several centuries [20]. Therefore, cycloastragenol, which is the major active compound in this plant, is of high interest to target liver diseases [21]. The evidence from our study revealed for the first time that cycloastragenol alleviated the progression of liver fibrosis resulting from chronic exposure to a hepatotoxin CCl₄. Moreover, we revealed that the hepatoprotective efficacy of cycloastragenol played a major role in the alleviation of fibrosis progression. Trichloromethyl free radical (CCl₃·), which is the toxic metabolite of CCl₄, induces liver damage by altered cellular integrity leading to swelling, cytolysis, and death of hepatocytes, and prolonged exposure of CCl₄ establish liver fibrosis [22,23]. Following the death of hepatocytes, several pro-inflammatory and pro-fibrotic mediators such as chemokine ligands/receptors and TGF-β1, respectively, are released to aggravate the initial damage in contiguous hepatocytes, Kupffer cells, and HSCs [24]. Despite unclear in-depth mechanisms, we found that cycloastragenol mitigated the toxicity of CCl₄, resulting in the reduction of leaked cytoplasmic liver enzymes in the serum. Furthermore, the hepatoprotective efficacy may contribute to the preserved metabolic function of the livers, since we found that the level of bilirubin which requires a phase II microsomal enzyme glucuronosyltransferase to be excreted [25] was reduced by cycloastragenol.

The resolution of excessive deposition of ECM is a pivotal function of Mmps, the master class of enzymes possessing protease activity that play a role in liver fibrogenesis [8]. Despite conventional dividends based on enzyme–substrate specificity and cellular locations, these proteases may be alternatively differentiated by their pathophysiological role into pro- and anti-fibrotic Mmps [26]. In our study, the level of a pro-fibrotic Mmp2 (gelatinase-A) [27] in the liver of mice who received cycloastragenol was slightly lower than mice treated with CCl₄ alone. In contrast, the levels of anti-fibrotic Mmp8 (collagenase-2), Mmp9 (gelatinase-B), and Mmp12 (metalloelastase) were markedly increased by cycloastragenol. Our findings were in line with several animal studies targeting fibrosis [28–30].

Among the quantification of multiple markers associated with inflammation, oxidative stress, and senescence, we found that CCl₄ significantly altered the mRNA expression of *Il6*. Even though *Il6* is usually recognized as a deleterious mediator, recent evidence demonstrated that this pleiotropic anti-inflammatory cytokine plays a vital role in the promotion of liver regeneration in liver pathologies [31]. Moreover, a previous study in mice treated with CCl₄ showed that a combination of *Il6* and mesenchymal stem cell transplantation attenuated liver fibrosis in mice [32]. Thus, cycloastragenol, which upregulated *Il6* in our study, could possibly promote hepatocyte regeneration after the damage of CCl₄. According to the effects on other markers using real-time quantitative PCR, anti-inflammatory activity would not be the main contributor to the hepatoprotective efficacy of cycloastragenol. Regarding markers of oxidative stress, the mRNA expression of *Nqo1* was increased by CCl₄. A previous study showed that this cytoprotective enzyme played a role in the detoxification of reactive species in livers obtained from patients with paracetamol overdose and primary biliary cholangitis [33]. Due to the fact that cycloastragenol did not significantly alter the expression of gene-encoding *Nqo1*, the antioxidant activity might be trivial for the beneficial efficacy of cycloastragenol in our study. Similarly, the anti-senescent activity of cycloastragenol may be negligible also. Nevertheless, cycloastragenol may possibly exhibit anti-fibrotic potency via anti-senescent activity in a case in which the experiment was performed in aged species [34].

Since we could not detect a significant alteration in the expression of transforming growth factor-beta receptor II, phosphorylated-Smad2 (pSmad2), pSmad3, and Smad4 resulting from CCl₄ exposure, the involvement of cycloastragenol on canonical TGF-β1 signaling could not be concluded. Although the canonical TGF-β1 signaling is usually recognized as the major activated pathway in liver fibrogenesis, a variety of responses in certain mouse strains against CCl₄ were reported [17,35]. In our ICR mice, it is possible that cycloastragenol regulated non-canonical pathways of TGF-β1 signaling, due to the levels of phosphorylated-Akt being slightly affected by CCl₄ and cycloastragenol. In addition, a previous study showed that an herbal extract ameliorated CCl₄-induced liver fibrosis in mice by inhibiting Akt-mediated hepatocyte apoptosis and regulating farnesoid X receptor (FXR) activity [36]. The effects of cycloastragenol on FXR could be gleaned from another study targeting hepatic steatosis in diet-induced obesity mice. This animal study administered cycloastragenol as a diet supplement at a dosage of 100 mg/100 g diet. Since the C57BL/6 mice at 30 g body weight consumed a 2.5–3 g diet per day, these mice could receive cycloastragenol at approximately 80–100 mg/kg dosage [37]. The results from these obesity mice showed that cycloastragenol improved fatty liver via FXR activation. Unfortunately, this study did not assess outcomes relating to fibrosis. Nevertheless, the effective anti-fibrotic dosage of cycloastragenol at 200 mg/kg in our study could sufficiently activate FXR. Since several previous studies demonstrated that FXR agonists impeded liver fibrosis and inhibited hepatocyte apoptosis [38–40], FXR activation might partly contribute to the anti-fibrotic efficacy of cycloastragenol. This dosage correlation might imply how the low dosage at 50 mg/kg of cycloastragenol, which was selected from a study targeting skin inflammation in psoriatic mice [41], could not be sufficient for modulating FXR and provided a clear anti-fibrotic efficacy in our study. Furthermore, the notch signaling that was modulated by astragaloside in the prevention of liver fibrosis in bile duct-ligated rats [12] might also connect with the anti-fibrotic efficacy of cycloastragenol.

Finally, it is worthwhile to mention that our study was performed on outbred mice. This fact could be considered as a limitation since a variation on the effects of CCl₄ and cycloastragenol might be relatively large as we demonstrated in an acute toxicity model of CCl₄ using these outbred mice [42]. On the other hand, although inbred mice are usually preferred in almost all biomedical research currently because of their reduced genetic variability, experiments in outbred mice may be considered a better choice since they consist of inter-individual genetic variation [43].

5. Conclusions

Cycloastragenol at the dosage of 200 mg/kg alleviated the progression of liver fibrosis in CCl₄-treated mice. The anti-fibrotic efficacy of cycloastragenol was mainly due to its hepatoprotection and was partly derived by the increased ECM resolution resulting from the upregulation of anti-fibrotic Mmps. Although the major mechanism of action required further elucidation, the inhibition of the non-canonical TGF-β1/Akt signaling pathway and possibly the modulation of FXR were supposed to play a role contributing to the anti-fibrotic and hepatoprotective potency of cycloastragenol.

Author Contributions: Conceptualization, T.L. and W.P.; investigation, formal analysis, and methodology, T.L., P.P., V.T. and W.P.; writing—original draft preparation, T.L.; writing—review and editing, P.O. and W.P.; supervision, P.O. and W.P.; project administration, T.L. and W.P.; funding acquisition, T.L. All authors have read and agreed to the published version of the manuscript.

Funding: This research was funded by the Specific League Funds from Mahidol University (IO86408204600).

Institutional Review Board Statement: This study was approved by the Animal Ethical Committee of the Faculty of Pharmacy, Mahidol University (PYR002/2021 and PYR008/2022).

Informed Consent Statement: Not applicable.

Data Availability Statement: The data presented in this study are available on request from the corresponding author.

Acknowledgments: This research paper is supported by Specific League Funds from Mahidol University. We would like to thank Wang Nguitrageol and Khajohnpong Manopwisedjaroen from Mahidol Vivax Research Unit (MVRU), Faculty of Tropical Medicine, Mahidol University, for technical assistances to perform PCR array.

Conflicts of Interest: The authors declare no conflict of interest.

References

1. D'souza, S.; Lau, K.C.; Coffin, C.S.; Patel, T.R. Molecular Mechanisms of Viral Hepatitis Induced Hepatocellular Carcinoma. *World J. Gastroenterol.* **2020**, *26*, 5759–5783. [[CrossRef](#)] [[PubMed](#)]
2. Lackner, C.; Tiniakos, D. Fibrosis and Alcohol-Related Liver Disease. *J. Hepatol.* **2019**, *70*, 294–304. [[CrossRef](#)] [[PubMed](#)]
3. Kolaric, T.O.; Nincevic, V.; Kuna, L.; Duspara, K.; Bojanic, K.; Vukadin, S.; Raguz-Lucic, N.; Wu, G.Y.; Smolic, M. Drug-Induced Fatty Liver Disease: Pathogenesis and Treatment. *J. Clin. Transl. Hepatol.* **2021**, *9*, 731–737. [[CrossRef](#)] [[PubMed](#)]
4. Wu, H.; Chen, C.; Ziani, S.; Nelson, L.J.; Ávila, M.A.; Nevzorova, Y.A.; Cubero, F.J. Fibrotic Events in the Progression of Cholestatic Liver Disease. *Cells* **2021**, *10*, 1107. [[CrossRef](#)] [[PubMed](#)]
5. Qu, W.; Ma, T.; Cai, J.; Zhang, X.; Zhang, P.; She, Z.; Wan, F.; Li, H. Liver Fibrosis and MAFLD: From Molecular Aspects to Novel Pharmacological Strategies. *Front. Med.* **2021**, *8*, 761538. [[CrossRef](#)] [[PubMed](#)]
6. Roehlen, N.; Crouchet, E.; Baumert, T.F. Liver Fibrosis: Mechanistic Concepts and Therapeutic Perspectives. *Cells* **2020**, *9*, 875. [[CrossRef](#)] [[PubMed](#)]
7. Kisseleva, T.; Brenner, D. Molecular and Cellular Mechanisms of Liver Fibrosis and Its Regression. *Nat. Rev. Gastroenterol. Hepatol.* **2021**, *18*, 151–166. [[CrossRef](#)]
8. Duarte, S.; Baber, J.; Fujii, T.; Coito, A.J. Matrix Metalloproteinases in Liver Injury, Repair and Fibrosis. *Matrix Biol.* **2015**, *44–46*, 147–156. [[CrossRef](#)]
9. Hoare, M.; Das, T.; Alexander, G. Ageing, Telomeres, Senescence, and Liver Injury. *J. Hepatol.* **2010**, *53*, 950–961. [[CrossRef](#)]
10. Dewidar, B.; Meyer, C.; Dooley, S.; Meindl-Beinker, A.N. TGF- β in Hepatic Stellate Cell Activation and Liver Fibrogenesis-Updated 2019. *Cells* **2019**, *8*, 1419. [[CrossRef](#)]
11. Yu, Y.; Zhou, L.; Yang, Y.; Liu, Y. Cycloastragenol: An Exciting Novel Candidate for Age-Associated Diseases. *Exp. Ther. Med.* **2018**, *16*, 2175–2182. [[CrossRef](#)] [[PubMed](#)]
12. Yongping, M.; Zhang, X.; Xuwei, L.; Fan, W.; Chen, J.; Zhang, H.; Chen, G.; Liu, C.; Liu, P. Astragaloside Prevents BDL-Induced Liver Fibrosis through Inhibition of Notch Signaling Activation. *J. Ethnopharmacol.* **2015**, *169*, 200–209. [[CrossRef](#)] [[PubMed](#)]
13. Zhou, Y.; Tong, X.; Ren, S.; Wang, X.; Chen, J.; Mu, Y.; Sun, M.; Chen, G.; Zhang, H.; Liu, P. Synergistic Anti-Liver Fibrosis Actions of Total Astragalus Saponins and Glycyrrhizic Acid via TGF- β 1/Smads Signaling Pathway Modulation. *J. Ethnopharmacol.* **2016**, *190*, 83–90. [[CrossRef](#)] [[PubMed](#)]
14. Kilkenny, C.; Browne, W.; Cuthill, I.C.; Emerson, M.; Altman, D.G. NC3Rs Reporting Guidelines Working Group Animal Research: Reporting in Vivo Experiments: The ARRIVE Guidelines. *Br. J. Pharmacol.* **2010**, *160*, 1577–1579. [[CrossRef](#)]
15. Lattouf, R.; Younes, R.; Lutomski, D.; Naaman, N.; Godeau, G.; Senni, K.; Changotade, S. Picrosirius Red Staining: A Useful Tool to Appraise Collagen Networks in Normal and Pathological Tissues. *J. Histochem. Cytochem.* **2014**, *62*, 751–758. [[CrossRef](#)] [[PubMed](#)]
16. Suvarna, S.K.; Layton, C.; Bancroft, J.D. (Eds.) *Bancroft's Theory and Practice of Histological Techniques*, 8th ed.; Elsevier: Amsterdam, The Netherlands, 2019; pp. 126–138.
17. Kim, Y.O.; Popov, Y.; Schuppan, D. Optimized Mouse Models for Liver Fibrosis. *Methods Mol. Biol.* **2017**, *1559*, 279–296. [[CrossRef](#)] [[PubMed](#)]
18. Zarrinpar, A.; Busuttill, R.W. Liver Transplantation: Past, Present and Future. *Nat. Rev. Gastroenterol. Hepatol.* **2013**, *10*, 434–440. [[CrossRef](#)]
19. Caligiuri, A.; Gentilini, A.; Pastore, M.; Gitto, S.; Marra, F. Cellular and Molecular Mechanisms Underlying Liver Fibrosis Regression. *Cells* **2021**, *10*, 2759. [[CrossRef](#)]
20. Shen, C.Y.; Jiang, J.G.; Yang, L.; Wang, D.W.; Zhu, W. Anti-Ageing Active Ingredients from Herbs and Nutraceuticals Used in Traditional Chinese Medicine: Pharmacological Mechanisms and Implications for Drug Discovery. *Br. J. Pharmacol.* **2017**, *174*, 1395–1425. [[CrossRef](#)]
21. Zhang, S.D.; Lu, J.; Yan, J.; Zhang, H. Research Progress of Preparation Technology and Pharmacological Effect of Cy-cloastragenol. *Chin. J. New Drugs* **2016**, *16*, 1872–1875.
22. Scholten, D.; Trebicka, J.; Liedtke, C.; Weiskirchen, R. The Carbon Tetrachloride Model in Mice. *Lab. Anim.* **2015**, *49*, 4–11. [[CrossRef](#)] [[PubMed](#)]
23. Weber, L.W.D.; Boll, M.; Stampfl, A. Hepatotoxicity and Mechanism of Action of Haloalkanes: Carbon Tetrachloride as a Toxicological Model. *Crit. Rev. Toxicol.* **2003**, *33*, 105–136. [[CrossRef](#)] [[PubMed](#)]
24. Kumar, S.; Duan, Q.; Wu, R.; Harris, E.N.; Su, Q. Pathophysiological Communication between Hepatocytes and Non-Parenchymal Cells in Liver Injury from NAFLD to Liver Fibrosis. *Adv. Drug Deliv. Rev.* **2021**, *176*, 113869. [[CrossRef](#)] [[PubMed](#)]
25. Fujiwara, R.; Haag, M.; Schaeffeler, E.; Nies, A.T.; Zanger, U.M.; Schwab, M. Systemic Regulation of Bilirubin Homeostasis: Potential Benefits of Hyperbilirubinemia. *Hepatology* **2018**, *67*, 1609–1619. [[CrossRef](#)] [[PubMed](#)]

26. Naim, A.; Pan, Q.; Baig, M.S. Matrix Metalloproteinases (MMPs) in Liver Diseases. *J. Clin. Exp. Hepatol.* **2017**, *7*, 367–372. [[CrossRef](#)] [[PubMed](#)]
27. Préaux, A.M.; Mallat, A.; Nhieu, J.T.; D’Ortho, M.P.; Hembry, R.M.; Mavier, P. Matrix Metalloproteinase-2 Activation in Human Hepatic Fibrosis Regulation by Cell-Matrix Interactions. *Hepatology* **1999**, *30*, 944–950. [[CrossRef](#)]
28. Siller-López, F.; Sandoval, A.; Salgado, S.; Salazar, A.; Bueno, M.; Garcia, J.; Vera, J.; Gálvez, J.; Hernández, I.; Ramos, M.; et al. Treatment with Human Metalloproteinase-8 Gene Delivery Ameliorates Experimental Rat Liver Cirrhosis. *Gastroenterology* **2004**, *126*, 1122–1133. [[CrossRef](#)]
29. Wu, Y.; Lu, S.; Huang, X.; Liu, Y.; Huang, K.; Liu, Z.; Xu, W.; Zhu, W.; Hou, J.; Liu, H.; et al. Targeting CIAPs Attenuates CCl₄-Induced Liver Fibrosis by Increasing MMP9 Expression Derived from Neutrophils. *Life Sci.* **2022**, *289*, 120235. [[CrossRef](#)]
30. Pellicoro, A.; Aucott, R.L.; Ramachandran, P.; Robson, A.J.; Fallowfield, J.A.; Snowdon, V.K.; Hartland, S.N.; Vernon, M.; Duffield, J.S.; Benyon, R.C.; et al. Elastin Accumulation Is Regulated at the Level of Degradation by Macrophage Metalloelastase (MMP-12) during Experimental Liver Fibrosis. *Hepatology* **2012**, *55*, 1965–1975. [[CrossRef](#)]
31. Naseem, S.; Hussain, T.; Manzoor, S. Interleukin-6: A Promising Cytokine to Support Liver Regeneration and Adaptive Immunity in Liver Pathologies. *Cytokine Growth Factor Rev.* **2018**, *39*, 36–45. [[CrossRef](#)]
32. Nasir, G.A.; Mohsin, S.; Khan, M.; Shams, S.; Ali, G.; Khan, S.N.; Riazuddin, S. Mesenchymal Stem Cells and Interleukin-6 Attenuate Liver Fibrosis in Mice. *J. Transl. Med.* **2013**, *11*, 78. [[CrossRef](#)]
33. Aleksunes, L.M.; Goedken, M.; Manautou, J.E. Up-Regulation of NAD(P)H Quinone Oxidoreductase 1 during Human Liver Injury. *World J. Gastroenterol.* **2006**, *12*, 1937–1940. [[CrossRef](#)] [[PubMed](#)]
34. Yu, Y.; Wu, J.; Li, J.; Liu, Y.; Zheng, X.; Du, M.; Zhou, L.; Yang, Y.; Luo, S.; Hu, W.; et al. Cycloastragenol Prevents Age-Related Bone Loss: Evidence in d-Galactose-Treated and Aged Rats. *Biomed. Pharmacother.* **2020**, *128*, 110304. [[CrossRef](#)] [[PubMed](#)]
35. McCracken, J.M.; Chalise, P.; Briley, S.M.; Dennis, K.L.; Jiang, L.; Duncan, F.E.; Pritchard, M.T. C57BL/6 Substrains Exhibit Different Responses to Acute Carbon Tetrachloride Exposure: Implications for Work Involving Transgenic Mice. *Gene Expr.* **2017**, *17*, 187–205. [[CrossRef](#)] [[PubMed](#)]
36. Jiang, M.; Huang, C.; Wu, Q.; Su, Y.; Wang, X.; Xuan, Z.; Wang, Y.; Xu, F.; Ge, C. Sini San Ameliorates CCl₄-Induced Liver Fibrosis in Mice by Inhibiting AKT-Mediated Hepatocyte Apoptosis. *J. Ethnopharmacol.* **2022**, *303*, 115965. [[CrossRef](#)]
37. Gu, M.; Zhang, S.; Zhao, Y.; Huang, J.; Wang, Y.; Li, Y.; Fan, S.; Yang, L.; Ji, G.; Tong, Q.; et al. Cycloastragenol Improves Hepatic Steatosis by Activating Farnesoid X Receptor Signalling. *Pharmacol. Res.* **2017**, *121*, 22–32. [[CrossRef](#)]
38. Schwabl, P.; Hambruch, E.; Seeland, B.A.; Hayden, H.; Wagner, M.; Garnys, L.; Strobel, B.; Schubert, T.-L.; Riedl, F.; Mitteregger, D.; et al. The FXR Agonist PX20606 Ameliorates Portal Hypertension by Targeting Vascular Remodelling and Sinusoidal Dysfunction. *J. Hepatol.* **2017**, *66*, 724–733. [[CrossRef](#)]
39. Wang, H.; Ge, C.; Zhou, J.; Guo, Y.; Cui, S.; Huang, N.; Yan, T.; Cao, L.; Che, Y.; Zheng, Q.; et al. Noncanonical Farnesoid X Receptor Signaling Inhibits Apoptosis and Impedes Liver Fibrosis. *EBioMedicine* **2018**, *37*, 322–333. [[CrossRef](#)]
40. Carino, A.; Cipriani, S.; Marchianò, S.; Biagioli, M.; Santorelli, C.; Donini, A.; Zampella, A.; Monti, M.C.; Fiorucci, S. BAR502, a Dual FXR and GPBAR1 Agonist, Promotes Browning of White Adipose Tissue and Reverses Liver Steatosis and Fibrosis. *Sci. Rep.* **2017**, *7*, 42801. [[CrossRef](#)] [[PubMed](#)]
41. Deng, G.; Chen, W.; Wang, P.; Zhan, T.; Zheng, W.; Gu, Z.; Wang, X.; Ji, X.; Sun, Y. Inhibition of NLRP3 Inflammasome-Mediated Pyroptosis in Macrophage by Cycloastragenol Contributes to Amelioration of Imiquimod-Induced Psoriasis-Like Skin Inflammation in Mice. *Int. Immunopharmacol.* **2019**, *74*, 105682. [[CrossRef](#)] [[PubMed](#)]
42. Luangmonkong, T.; Pransin, C.; Noppahalee, L.; Meechai, S.; Chunya, S.; Rattanavaraha, A.; Kaewnoppharat, N.; Khuituan, T.; Bunyakiat, S.; Parichatikanond, W. Carbon Tetrachloride-Induced Acute Liver Toxicity: Selecting Dosage and Biomarkers for Evaluating Hepatoprotective Drugs in ICR Outbred Mice. *Pharm. Sci. Asia* **2022**, *49*, 534–542. [[CrossRef](#)]
43. Tuttle, A.H.; Philip, V.M.; Chesler, E.J.; Mogil, J.S. Comparing Phenotypic Variation between Inbred and Outbred Mice. *Nat. Methods* **2018**, *15*, 994–996. [[CrossRef](#)] [[PubMed](#)]

Disclaimer/Publisher’s Note: The statements, opinions and data contained in all publications are solely those of the individual author(s) and contributor(s) and not of MDPI and/or the editor(s). MDPI and/or the editor(s) disclaim responsibility for any injury to people or property resulting from any ideas, methods, instructions or products referred to in the content.